Journal of Medicinal Chemistry

Article

Multi-target-directed Benzylidene-indanone derivatives: Anti-# Amyloid (A#) aggregation, Antioxidant, Metal chelation and Monoamine oxidase B (MAO-B) Inhibition Properties Against Alzheimer's disease

Ling Huang, Chuanjun Lu, Yang Sun, Fei Mao, Zonghua Luo, Tao Su, Huailei Jiang, Wenjun Shan, and Xingshu Li

J. Med. Chem., **Just Accepted Manuscript** • Publication Date (Web): 14 Sep 2012

Multi-target-directed Benzylidene-indanone derivatives: Anti-β Amyloid (Aβ) aggregation, Antioxidant, Metal chelation and Monoamine oxidase B (MAO-B) Inhibition Properties Against Alzheimer's disease

Ling Huang, Chuanjun Lu, Yang Sun, Fei Mao，Zonghua Luo，Tao Su, Huailei Jiang, Wenjun Shan, Xingshu Li*

Institute of Drug Synthesis and Pharmaceutical Processing, School of Pharmaceutical Sciences, Sun Yat-sen University, Guangzhou 510006, China

ABSTRACT

A novel series of benzylidene-indanone derivatives were designed, synthesised and evaluated as multi-target-directed ligands against Alzheimer's disease. The in vitro studies showed that most of the molecules exhibited a significant ability to inhibit self-induced Aβ aggregation (10.5-80.1%, 20 μM) and MAO-B activity (IC_{50} of 7.5-40.5μM), to act as potential antioxidants (ORAC-FL value of 2.75-9.37), and to function as metal chelators. In particular, compound **41,** had the greatest ability to inhibit Aβ aggregation (80.1%) and MAO-B (IC_{50}=7.5μM), was also an excellent antioxidant and metal chelator. Moreover, it is capable of inhibiting Cu(II)-induced **A**β aggregation and disassembling the well-structured Aβ fibrils. These results indicated that compound **41** is an excellent multifunctional agent for the treatment of AD.

Introduction

Alzheimer' disease (AD) is a multifaceted, progressive neurodegenerative disorder characterised by progressive cognitive decline and memory loss. Although the etiology of AD is not fully known at present, several conditions have been considered to play significant roles in the pathogenesis of AD. These include the development of deposits of β-amyloid and τ-protein, oxidative stress, dyshomeostasis of biometals, and low levels of acetylcholine (ACh).[1] In particular, the production and accumulation of oligomeric aggregates of Aβ in the brain are a central event in the pathogenesis of AD according to the "amyloid hypothesis" as they are thought to be able to initiate the pathogenic cascade, ultimately leading to neuronal loss and dementia.[2] Aβ can efficiently generate reactive oxygen species in the presence of some transition metals and form stable dityrosine cross-linked dimers, which are generated by free radical attack under oxidative conditions.[3] Oxidative damage is present within the brain of AD patients, and it was shown to affect every class of biological macromolecules, including nucleic acids, proteins, lipids, and carbohydrates.[4] It is also an event that precedes the appearance of other pathological hallmarks of the disease, such as amyloid plaques and neurofibrillary tangles.[5,6] Therefore, antioxidant protection is important during aging and especially in AD patients as the endogenous antioxidant protection system declines rapidly.

Monoamine oxidases A and B (MAO-A and MAO-B) are important FAD-dependent enzymes (flavoenzymes) responsible for the metabolism of neurotransmitters such as dopamine, serotonin, adrenaline, and noradrenaline and for

the inactivation of exogenous arylalkylamines.[7] Thus, the inhibition of MAO -A/MAO-B increases, primarily in the CNS, the levels of such neurotransmitters, which are decreased in AD patients compared to age-matched controls.[8] Selegiline, a selective MAO-B inhibitor, has been shown to significantly improve learning and memory deficits in animal models associated with AD and to slow the disease progression in AD patients.[9] This evidence suggested that selective MAO-B inhibitors seem to be an important treatment of AD.

Recently, transition metals, including copper and zinc, have been found to directly bind to amyloid plaques by spectroscopic studies.[10,11] Moreover, studies suggested that redox-active metal ions, such as Cu^{2+} and Fe^{2+}, are involved in the production of reactive oxygen species (ROS) and oxidative stress,[12] which implies that these biometals also play a central role in many critical aspects of AD. Thus, modulation of such biometals in the brain has been proposed as a potential therapeutic strategy for the treatment of AD.[13]

The multifaceted conditions of the AD state have encouraged active research in the development of multi-target-directed ligands (MTDLs) to act as agents for the treatment of this disease.[14,15,16,17] These drugs, which possess two or more complementary biological activities, may represent an important clinical advance in the future.

Indanones and their derivatives are important bioactive molecules that have been studied to determine their biological activities within disease states, including Alzheimer's disease and cancer. For example, gallic acid-based indanone (**1**, Fig. 1)

derivatives and some imidazolyl-substituted 2-benzylidene indanone derivatives were recently studied as inhibitors for cancer treatment.[18] Indanocine (**2**, Fig. 1) and its analogues were developed to combat drug-resistant malignancies.[19] Donepezil hydrochloride (**3**, Fig. 1), which acts as an AChE inhibitor, was approved by the FDA for the treatment of mild to moderate Alzheimer's disease.[20]

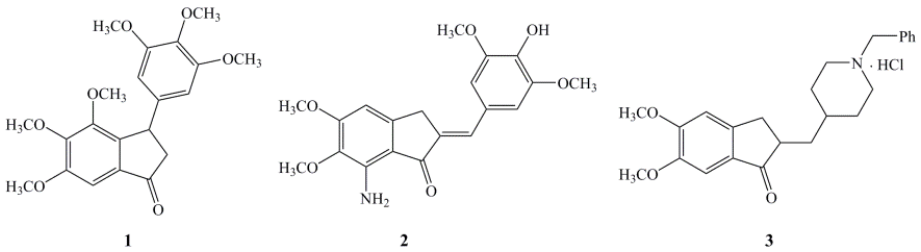

Figure 1: Some Indanone derivatives with important bioactivities

Previously, we reported the design, synthesis and evaluation of 9-O and 9-N substituted berberine derivatives as dual or multifunctional agents for the treatment of Alzheimer's disease.[21,22] In this paper, we report the study of the design, synthesis, and evaluation of a novel series of indanone derivatives that were found to show potentially applicable biological activities, including the inhibition of self-induced Aβ aggregation, inhibition of MAO-B activity, antioxidant properties and metal chelation.

Results and Discussion

Chemistry

The synthetic route of key intermediates **7-9** and **11-18** is shown in Scheme 1. The protection of hydroxy groups at the phenyl ring of **4-6** provided the THP-protected aromatic aldehyde derivatives **7-9**. The substitution of the fluorine atom of 4-fluoro benzaldehyde with a series of amines in the presence of TBAB gave intermediates

11-16. In compounds **17-18**, the aldehydes with a substituted amino group at the 4-position were converted to **11-12** by aminomethylation with formaldehyde and formic acid in reflux.

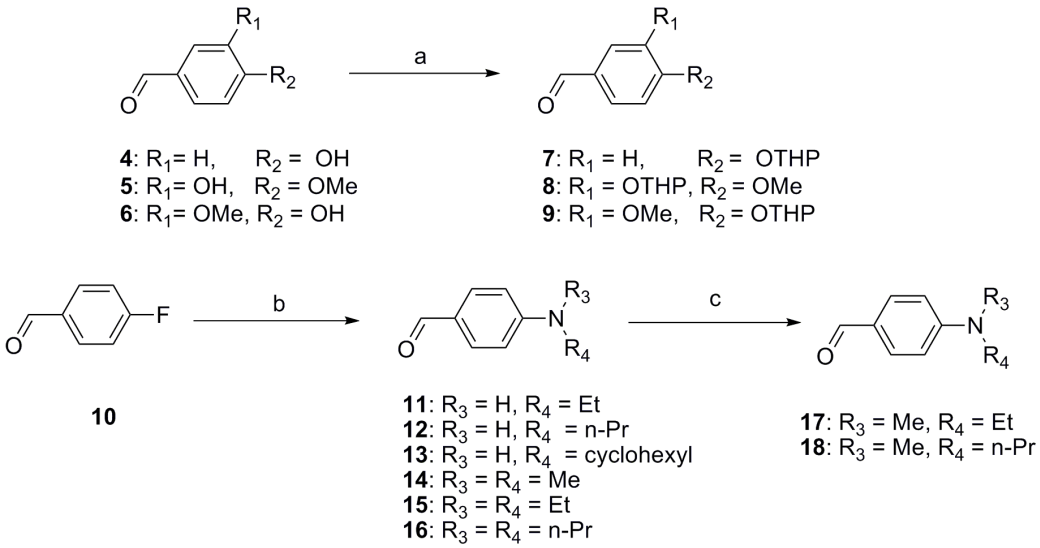

Scheme 1. Synthesis of the aromatic aldehyde intermediates **7-9** and **11-18**. Reagents and conditions: (a) 3,4-2H-Dihydropyran, PPTS, DCM, rt; (b) R_3NR_4, TBAB, K_2CO_3, DMSO, 90□; (c) 37% HCHO, HCOOH, reflux.

According to Scheme 2, **20** was synthesised by the reaction of 5,6-dimethoxy-1-indanone with boron tribromide in dichloromethane, which then reacted with iodomethane in the presence of lithium carbonate to provide 6-hydroxy-5-methoxyl-1-indanone, **21**. The reaction of compound **21** with 3,4-2H-dihydropyran afforded the THP-protected indanone derivative **22**. The target compounds **23-24**, without the hydroxy group on indanone or aldehyde segment, were obtained by direct condensation of the commercially available 5,6-dimethoxy-1-indanone (**19**) and the appropriate aldehydes in ethanolic KOH solution. Condensation of 5,6-dihydroxy-1-indanone (**20**) and corresponding amine,

catalysed by TsOH, gave compounds **38-41**. Finally, compounds **25-37** were obtained by the condensation of THP-protected indanone (**22**) with the appropriate benzaldehyde in ethanolic KOH solution, followed by removal of the THP protection.

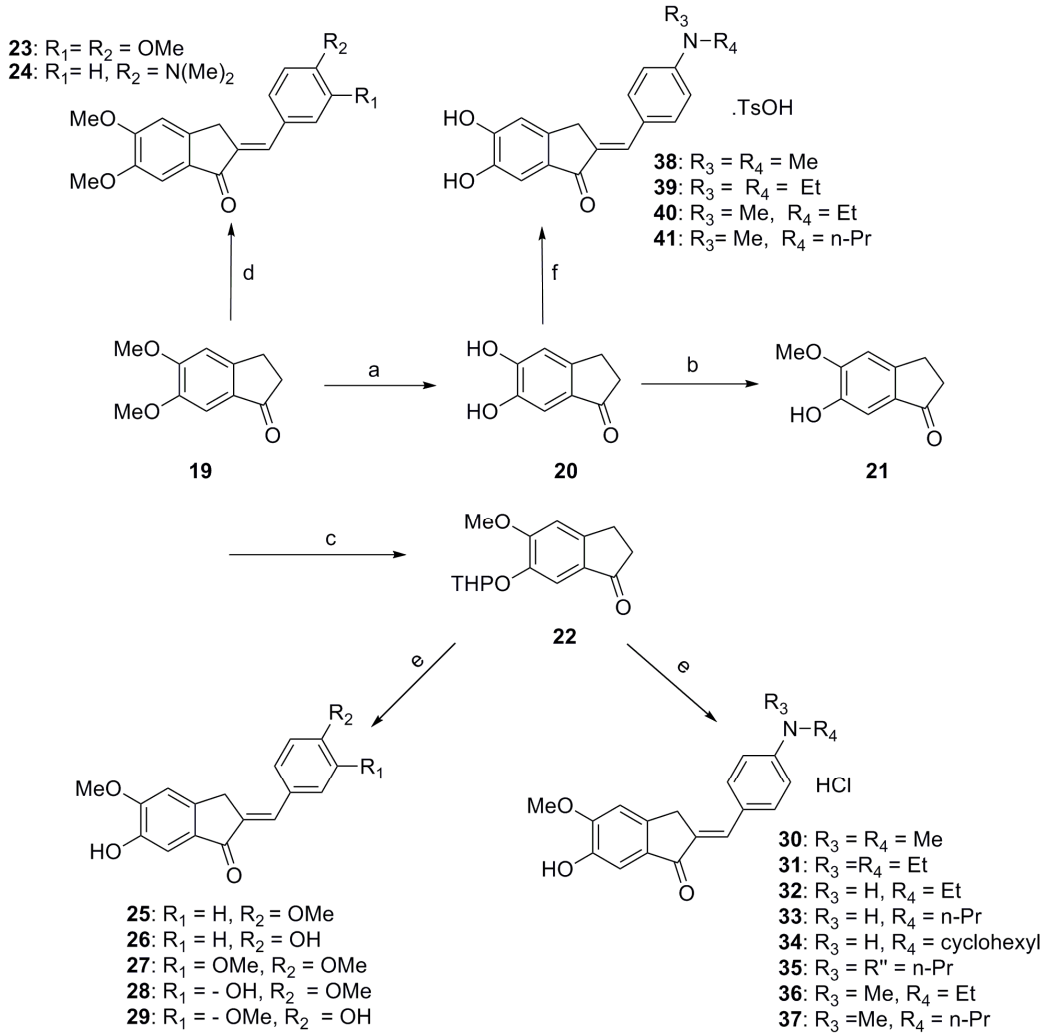

Scheme 2. Synthesis of target compounds **23-41**. Reagents and conditions: (a) BBr_3, DCM, -78°C; (b) Li_2CO_3, MeI, DMF, 55°C;(c) 3,4-2H-Dihydropyran ,PPTS, DCM, rt; (d) appropriate benzaldehyde, 4%KOH, EtOH, rt; (e) (i) appropriate benzaldehyde, 4%KOH, EtOH, rt; (ii) 2M HCl, EA/butanone-2, reflux. (f) appropriate benzaldehyde, TsOH, reflux.

Inhibition of self-mediated $A\beta_{1-42}$ aggregation

The ability of the indanone derivatives to inhibit $A\beta_{1-42}$ aggregation was assessed using the thioflavin T (ThT) fluorescence assay[23] with curcumin as standard. The results summarised in Table 1 showed that most indanone derivatives exhibited moderate-to-good potencies compared to that of curcumin. The optimal $A\beta_{1-42}$ aggregation inhibition potency (80.1%) was provided by compound **41** that features two hydroxy groups at the 5- and 6-positions of the indanone moiety (A ring) and one methyl(propyl)amino substitution at the 4-position of the aldehyde (B ring). These substituted groups seem to play an important role in the inhibition of Aβ aggregation. As indicated in Table 1, compound **23**, with four methoxy groups on the A and B ring, gave the lowest inhibitive activity (10.5%). De-methylation in different position in part led to a slight increase of the inhibitory activity for several compounds (14.2-28.4%). It is interesting that most of the substituted amino groups at the 4-position of the B ring (R^4) generally gave better results of the inhibitive activity 23.7-80.1%), with the exception of compounds **32** and **34** (NHEt, 10.5%, NHcyc-Hex, 16.8%). Compound **24,** featuring two hydroxy groups at 5- and 6-position of the A ring and one diethylamino group at the 4-position of B ring, gave 23.7% inhibition activity. On the other hand, compound **30**, with a hydroxy at 6-position of A ring, led to 33.8% inhibition. These results imply that the methoxy group is not favourable for inhibition activity. Fixation of the A ring with a 5-methoxy-6-hydroxy substitution of the amino groups also led to changes in measured inhibitory activity (compound **31**, diethylamino group at the 4-position of the B ring, 40.7%; compound **33**,

propylamino group, 38.4%, and others). Compounds **38-41**, with two hydroxy groups on the A ring, gave 61.4% - 80.1% inhibitory activity, which suggested that the two hydroxy groups at the 5- and 6-positions of the A ring seem to be beneficial to their activity.

Table 1. Inhibition of $A\beta_{1-42}$ aggregation and Oxygen Radical Absorbance Capacity (ORAC, Trolox Equivalents) by Curcumin and benzylidene-indanone derivatives **23-41**.

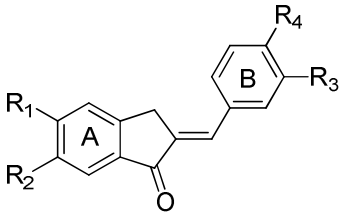

Comp.	R_1	R_2	R_3	R_4	Inhibition of $A\beta_{1-42}$ aggregation(%)[a]	ORAC[b]
Curcumin	-	-	-	-	52.1±2.7	2.57±0.17
23	OMe	OMe	OMe	OMe	10.5±0.4	0.65±0.04
24.HCl	OMe	OMe	H	$N(Me)_2$	23.7±0.7	7.85±0.68
25	OMe	OH	H	OMe	28.4±0.9	4.83±0.31
26	OMe	OH	H	OH	16.3±0.5	9.37±0.59
27	OMe	OH	OMe	OMe	19.5±1.0	4.55±0.26
28	OMe	OH	OH	OMe	24.0±1.3	3.55±0.20
29	OMe	OH	OMe	OH	14.2±0.7	6.58±0.55
30.HCl	OMe	OH	H	$N(Me)_2$	33.8±1.3	7.90±0.52
31.HCl	OMe	OH	H	$N(Et)_2$	40.7±1.6	3.96±0.33

32.HCl	OMe	OH	H	NHEt	10.5±0.3	4.75±0.39
33.HCl	OMe	OH	H	NHPr	38.4±1.1	4.14±0.40
34.HCl	OMe	OH	H	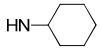	16.8±0.5	3.60±0.25
35.HCl	OMe	OH	H	$N(Pr)_2$	38.0±1.5	2.75±0.11
36.HCl	OMe	OH	H	NMeEt	42.1±2.0	5.34±0.23
37.HCl	OMe	OH	H	NMePr	50.0±2.4	5.11±0.38
38.TsOH	OH	OH	H	$N(Me)_2$	61.4±1.9	5.63±0.44
39.TsOH	OH	OH	H	$N(Et)_2$	67.0±3.8	5.41±0.26
40.TsOH	OH	OH	H	NMeEt	74.4±2.9	5.87±0.41
41.TsOH	OH	OH	H	NMePr	80.1±4.0	5.60±0.59

[a]The Thioflavin-T fluorescence method was used. Values are expressed as the mean ± SD from at least two independent measurements. All values were obtained at the concentration of 20 μM of the tested compounds.

[b]The mean ± SD of the three independent experiments, data are expressed as μ mol of trolox equivalent/μ mol of tested compound

Effects on abundance of Aβ fibrils by compound 41

To complement the ThT binding assay, $A\beta_{1-42}$ aggregation was also monitored by transmission electron microscopy (TEM) (Figure 2.). The results showed that the sample of $A\beta_{1-42}$ alone had aggregated into amyloid fibrils after 24 h incubation, while only small bulk aggregates were visible and no characteristic fibrils were observed in the sample of $A\beta_{1-42}$ in presence of **41**. The TEM results were well

consistent with the results of ThT measurements, which strongly proved that **41** can inhibit the $A\beta_{1-42}$ fibrils formation.

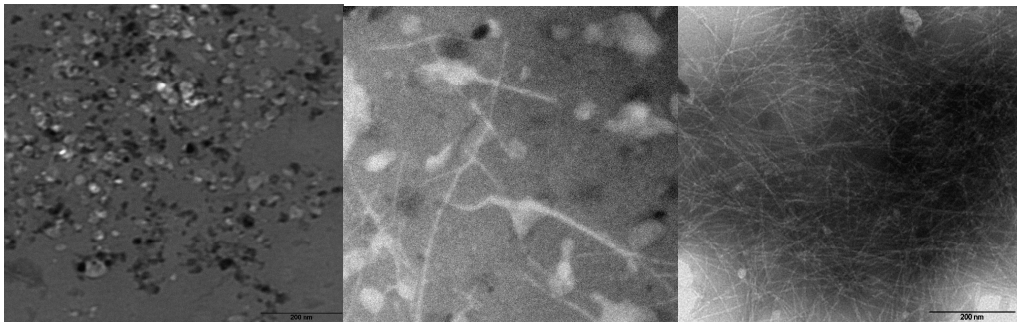

Aβ (0h) Aβ+ **41** (24h) Aβ alone (24h)

Figure 2. TEM images of $A\beta_{1-42}$(20μM) in the presence and absence of 20μM compound **41** after 24 h of aggregation.

Anti-oxidant activity in vitro

The antioxidant activity of the benzylidene-indanone derivatives were determined by an oxygen radical absorbance capacity assay that uses fluorescein (ORAC-FL), according to the method originally described by Ou *et al.* [24,25] and further modified by Dávalos *et al.*[26] Trolox, a vitamin E analogue, was used as a standard, and the antioxidant activity was expressed as Trolox equivalents (μmol of Trolox/μmol of tested compound). As shown in Table 1, most of the target compounds demonstrated good to excellent antioxidant activity with ORAC-FL values of 2.60–9.37 Trolox equivalents. Upon comparison of the ORAC-FL values of compound **23** with that of the other compounds, it is apparent that the free hydroxy or amino substituents are crucial to the radical scavenging ability.

Inhibition of MAOs *in vitro*

To further study the multipotent biological profile of the target compounds, the inhibitory activity against MAO-A and MAO-B (recombinant human enzyme) was determined and compared with that of Ladostigil, which was an MAO-B inhibitor approved to carry out phase II clinical trial by FDA. As shown in Table 2, most of the indanone derivatives were effective in inhibiting MAO-B in the micromolar range. Compound **41**, the most potent MAO-B inhibitors, with the IC_{50} of 7.50μM, is about 5-fold more potent than ladostigil. However, when the hydroxy groups at the 5-position of the A ring replaced by methoxy group (compound **37**), the inhibitory activity to both MAO-A (4.3% at 50μM) and MAO-B (IC50=40.5μM) decreased dramatically, which indicated that the hydroxy groups at the 5- position of A ring is critical to the activity.

Table 2. Inhibitory activity of typical molecules with human recombinant MAO isoforms and selectivity indices (SI)

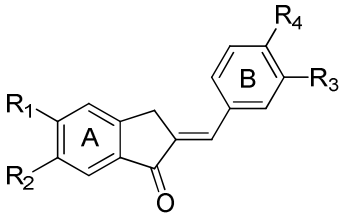

Comp.	R_1	R_2	R_3	R_4	$IC_{50}(\mu M)^a$		SI^b
					MAO-A	MAO-B	
31.HCl	OMe	OH	H	$N(Et)_2$	19.3%[c]	18.55±1.1	-
36.HCl	OMe	OH	H	NMeEt	14.4%[c]	28.7±1.7	-

37.HCl	OMe	OH	H	NMePr	4.3%[c]	40.5±3.0	-
38.TsOH	OH	OH	H	$N(Me)_2$	38.5±2.4	10.90±0.8	3.53
39.TsOH	OH	OH	H	$N(Et)_2$	41.4±3.1	7.71±0.5	5.36
40.TsOH	OH	OH	H	NMeEt	35.2±0.9	10.7±0.3	3.29
41.TsOH	OH	OH	H	NMePr	37.7±2.2	7.50±0.9	5.03
clorgyline	-	-	-	-	4.1±0.2nM	n.t.	-
ladostigil	-	-	-	-	n.t.	37.1±3.1	-
selegiline	-	-	-	-	70.2±3.8	18.5±2.1nM	37945
rasagiline	-	-	-	-	0.7[d]	0.014[d]	50

[a]All IC_{50} values shown in this Table are the mean ±SEM from three experiments.

[b]hMAO-B selectivity index = IC_{50} (hMAO-A)/IC_{50}(hMAO-B).

[c]The inhibition rate of compounds to MAO-A at 50μM.

[d] Reference 27

Docking study of compound 41 to MAO-B

In order to evaluate the binding modes of this class of indanone derivatives with respect to human MAO-B， docking simulations were carried out using the CDOCKER program in the Discovery studio 2.1 software based on the X-ray crystal structure of human MAO-B (PDB entry 2Z5X). Based on the in vitro inhibition results, we selected compound **41**, the highest MAO-B inhibitor, as a typical ligand for the evaluation. As shown in Figure 3 and 4, the indanone moiety of compound **41** close to the FAD cofactor, adopting parallel π-π interactions with Tyr398 (4.45 Å).

There were two hydrogen bonds between indanon moiety and FAD cofactor (FAD-NH…41-O11；41-OH…FAD-O), which could explain the critical function of hydroxy groups at the 5- position of A ring. Meanwhile, the benzene amine group interact with many hydrophilic acids, such as Phe168, Pro 115, Ser200, Leu 187, ILe199, Thr 131 and so on.

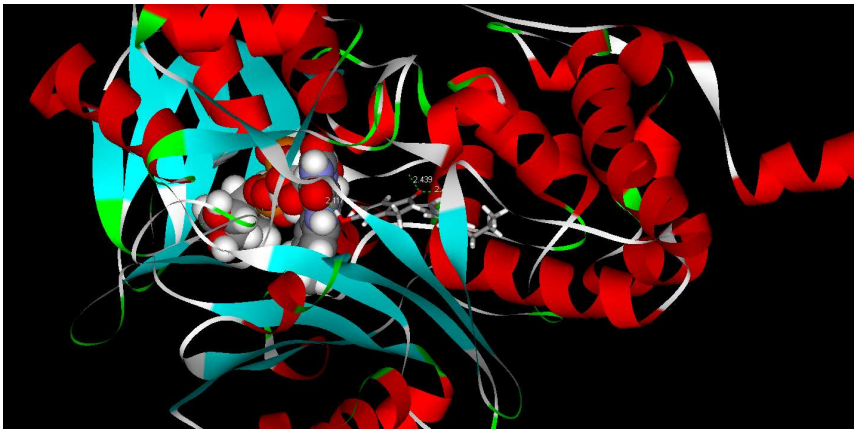

Figure 3: Predicted positions of **41** into hMAO-B catalytic sites. Compound **41** and The FAD cofactor were depicted using stick and space fill representation respectively.

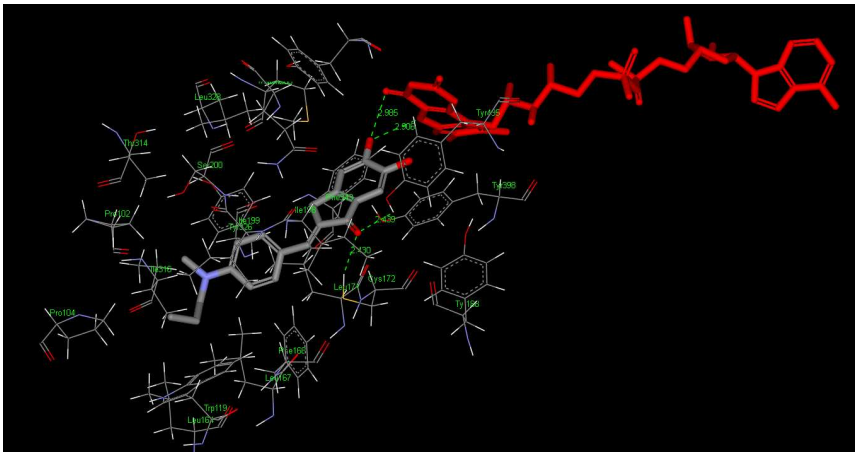

Figure 4: Representation of compound **41** docked into the binding site of MAO-B highlighting the protein residues that form the main interactions with the inhibitor. Hydrogen-bonding interaction between ligand and residues are shown with the green line.

Metal binding properties of compound 41

The chelation ability of compound **41** toward biometals such as Cu(□), Fe(□) and Zn(□) was studied by UV-vis spectrometry (Figure 5). When adding $CuSO_4$, the maximum absorption at 437nm exhibited a red shift to 451nm, which indicated the formation of **41**-Cu(□). However, with the addition of $FeSO_4$ and $ZnCl_2$, there was no significant shift. Interestingly, after adding $FeSO_4$, the absorption at 437 nm decreased obviously, which indicated that there was a possible interaction between **41** and Fe(□).

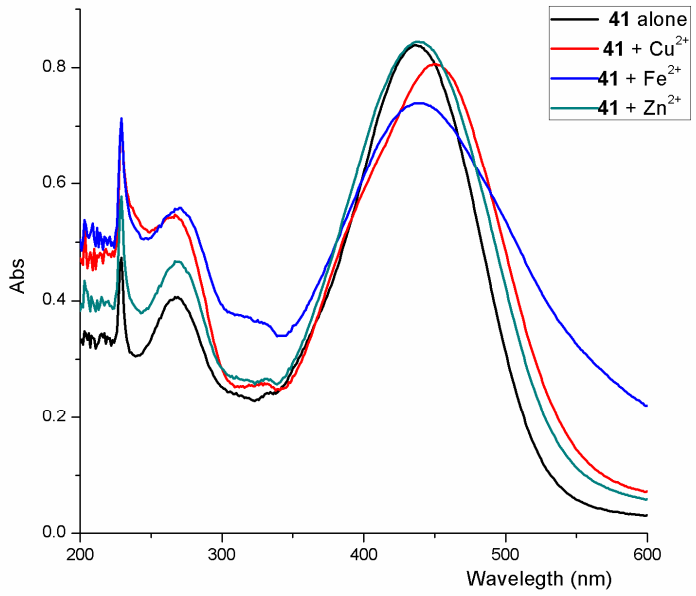

Figure 5. UV spectrum of compound 41 (50μM) alone or at the presence of 50μM $ZnSO_4$, $CuSO_4$, and $FeSO_4$.

To determine the stoichiometry of the complex **41**-Cu(□), the molar ratio method was used by preparing solutions of compound **41** with ascending amounts of $CuSO_4$. The UV spectra were performed to obtain the absorbance of the complex of $CuSO_4$ and **41** at different concentrations at 451nm. According to the Figure 6, the absorbance linearly increased at first. When the mole fraction of Cu(□) to **41** was more then 0.8, the absorbance tended to be stable. Therefore, two straight lines were drawn with the intersection point at a mole fraction of 0.8, revealing a 1:1 stoichiometry for complex **41**-Cu(□).

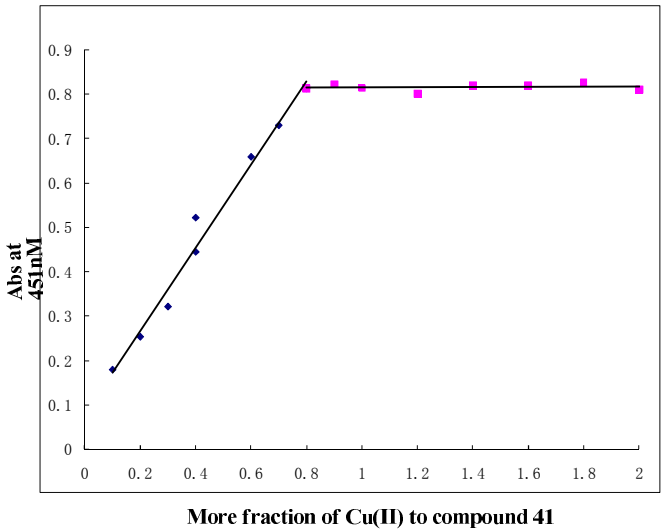

Figure 6: Determination of the stoichiometry of complex **41**-Cu(II) by molar ration method.

Effects on metal-induced $A\beta_{1-42}$ aggregation by compound 41

In order to investigate the effects of **41** on Cu(II)-induced Aβ aggregation, we carried out two individual studies (Figure 7 and Figure 8): inhibition activity of metal-induced $A\beta_{1-42}$ aggregation by compound **41** and disaggregation effects of **41** on

Cu(II)-induced $A\beta_{1-42}$ aggregates. ThT binding assay and transmission electron microscopy (TEM) were be used to identify the degree of Aβ aggregation.

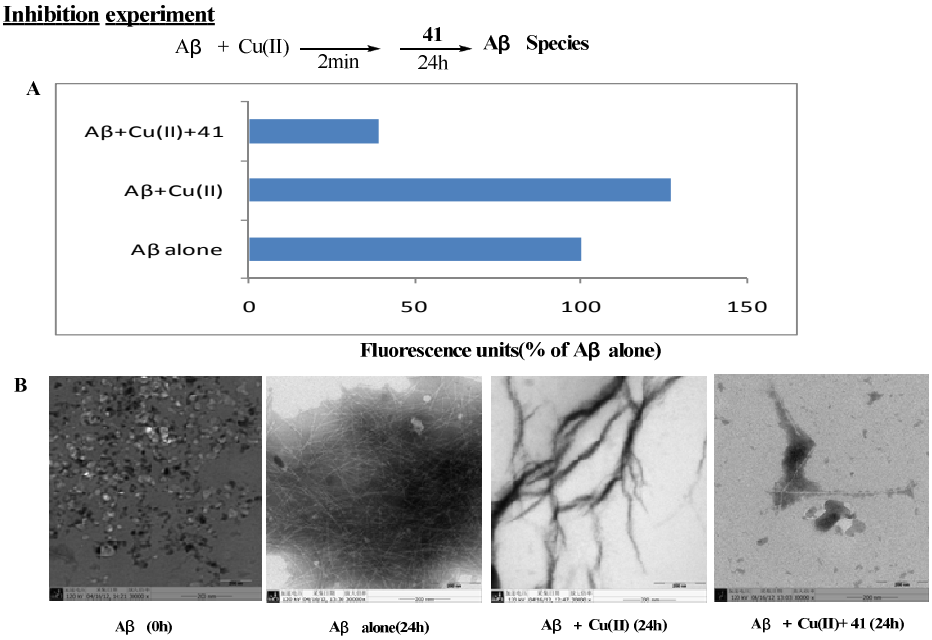

Figure 7: Visualization of Aβ species from inhibition experiments. Top: Scheme of the inhibition experiment . Bottom: (A) the results of ThT binding assay; (B)TEM images of samples.

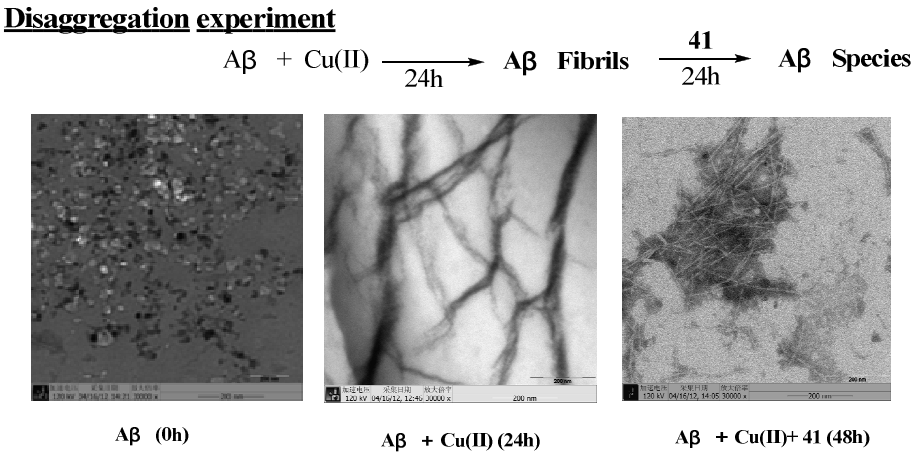

Figure 8: Visualization of Aβ species from disaggregation experiments. Top: Scheme of the disaggregation experiment . Bottom: TEM images of samples.

As shown in Figure 7, Cu(II) could accelerate the aggregation of Aβ. However, the rate of Aβ aggregation slowed down when adding **41** to the samples, which suggested that **41** could inhibited Cu(II)-induced **A**β aggregation noticeably through chelating with Cu(II). The results of TME are consistent with ThT binding assay results. For the disaggregation studies (Figure 8), **41** (50 μM) was added to Aβ fibrils generated by reacting Aβ (50 μM) with 1 equiv of Cu(II) (50 μM) for 24 h at 37°C with constant agitation. The TME figures illustrated that much fewer Aβ aggregates were observed after adding **41**, which indicated that **41** is able to alter the structure of metal-triggered Aβ aggregates affording their disaggregation. In short, based on these TEM results, we can conclude that compound **41** is capable of inhibiting Cu(II)-induced **A**β aggregation and disassembling the well-structured Aβ fibrils.

Conclusion

In conclusion, most benzylidene-indanone derivatives exhibited multifunctional activity as potential anti-AD drugs, which include significant ability to inhibit self-induced Aβ aggregation and MAO-B activity, to act as antioxidants and bio-metal chelators. Among the synthesised compounds, compound **41**, 5,6-dihydroxy-2-(4-(methyl(propyl)amino)benzylidene)-2,3-dihydro-1H-inden-1-one 4-methylbenzenesulfonate, gave the greatest inhibitory potency towards self-induced Aβ aggregation (80.1%, 20 μM), which was proved by TEM. Meanwhile, this compound was also an excellent antioxidant (ORAC-FL value of 5.60) and MAO-B inhibitor (IC_{50}=7.5μM). UV-vis spectrometry and TME results confirmed that compound **41** is not only a good bio-metal chelator by inhibiting Cu(II)-induced Aβ

aggregation, but also could disassemble the well-structured Aβ fibrils. Such multifunctional properties highlight compound **41** as interesting candidate for further studies directed to the development of novel drugs in the treatment of AD.

Experimental Section

General Information. The ^{1}H NMR and ^{13}C NMR spectra were recorded using TMS as the internal standard on a Bruker BioSpin GmbH spectrometer at 400.132 MHz and 100.614 MHz, respectively. Coupling constants are given in Hz. MS spectra were recorded on an Agilent LC-MS 6120 instrument with an ESI and APCI mass selective detector. High-resolution mass spectra were obtained using a Shimadzu LCMS-IT-TOF mass spectrometer. Flash column chromatography was performed using silica gel (200–300 mesh) purchased from Qingdao Haiyang Chemical Co. Ltd or alumina from Sinopharm Chemical Reagent Co. Ltd. All the reactions were monitored by thin layer chromatography using silica gel. The purity of compounds **23-41** (higher than 95%) was confirmed through HPLC (Agilent technologies 1200 series system, TC-C18 column (4.6×250 mm, 5μm), eluted with methanol/water (0.1% TFA), 75:25, at a flow rate of 0.5 mL/min).

General procedure for the preparation of 7-9

To the solution of **4, 5** or **6** (1mmol) and PPTS (1.5mmol) in DCM (10ml), 3,4-*2H*-dihydropyran (1.5mol) was added. The mixture was stirred for 10h and

concentrated in vacuum. The crude residue was purified by flash chromatography on a silica gel to furnish the oil products **7-9.**

General procedure for the preparation of 11-16

The mixture of 4-fluorobenzaldehyde (**10**, 2mmol), TBAB (1mmol), K_2CO_3 (2mmol) and the appropriate amine (10mmol) in DMSO was heated at 90□ for 20h. After cooled to room temperature, the mixture was diluted with 50ml water, and then extracted with ethyl acetate (50ml x 3). The combined organic phase was washed by water (10ml), brine (10ml), dried over Na_2SO_4, filtered and concentrated in vacuum to give the crude product which was purified by flash chromatography on a silica gel to furnish the oil products **11-16.**

General procedure for the preparation of 17-18

The mixture of **11-12** (1mmol), formaldehyde (5mmol) and formic acid (3mmol) was refluxed for 3h and concentrated in vacuum. The crude product was purified by flash chromatography on a silica gel to furnish the oil products **17-18.**

5,6-dihydroxy-2,3-dihydro-1H-inden-1-one (20)

BBr_3 (6mmol) was added slowly to the mixture of 5,6-dimethoxy-1-indanone (**19**, 2mmol) in 20ml DCM at -78□. After 3h, the mixture was cooled to room temperature, stirred for 1h and then water (50ml) was added to provide a red solid, which was filtered and dried to yield **20**.

6-hydroxy-5-methoxy-2,3-dihydro-1H-inden-1-one (21)

Li_2CO_3 (2mmol) and MeI (2.5mmol) were added to a solution of **20** (2mmol) in 15 ml DMF. The mixture was stirred at 55□ for 3h and cooled to room temperature. Ethyl acetate (150 mL) was added to the mixture and the organic phase was washed by water (50ml x 3), brine (10ml), dried over Na_2SO_4, filtered and concentrated in vacuum to furnish a yellow solid **21.**

5-methoxy-6-(tetrahydro-2H-pyran-2-yloxy)-2,3-dihydro-1H-inden-1-one (22)

3,4-2H-dihydropyran (1.5mol) was added to a solution of **20** (1mmol) and PPTS (1.5mmol) in DCM (10ml). The mixture was stirred for 10h, and concentrated in vacuum. The crude product was purified by flash chromatography on a silica gel to furnish the oil products **22.**

General procedure for the preparation of 23-24

5ml 4% KOH was added to a solution of 5,6-dimethoxy-1-indanone (**19**) (384mg, 2mmol) with the appropriate benzaldehyde (2mmol) in 5ml EtOH. After stirred at room temperature for 2-5 h, the solid was filtered, washed with water, and crystallized from methanol.

2-(3,4-dimethoxybenzylidene)-5,6-dimethoxy-2,3-dihydro-1H-inden-1-one (23)

5,6-dimethoxy-1-indanone (**19**) was treated with 3,4-dimethoxybenzaldehyde according to general procedure to give the desired product **23** as a yellow solid, 83% yield. Mp=195.6-196.3□; ^{1}H NMR (400 **MHz**, $CDCl_3$) δ 7.54 (s, 1H), 7.34 (s, 1H), 7.30 – 7.25 (m, 1H), 7.17 (d, *J* = 1.7 Hz, 1H), 6.99 (s, 1H), 6.94 (d, *J* = 8.4 Hz, 1H),

4.00 (s, 2H), 3.97 – 3.93 (m, 12H); ^{13}C NMR (101 MHz, $CDCl_3$) δ 194.37, 155.26, 149.64, 144.52, 133.36, 132.52, 131.26, 128.63, 124.37, 113.34, 111.32, 107.21, 105.10, 56.26, 55.97, 32.06; LCMS (APCI) m/z $[(M+H)]^+$ = 341.4; HRMS (ESI) m/z calcd for $C_{20}H_{20}O_5$, 341.1384. found, 341.1378; Purity: 95.1% (by HPLC).

2-(4-(dimethylamino)benzylidene)-5,6-dimethoxy-2,3-dihydro-1H-inden-1-one (24)

5,6-dimethoxy-1-indanone (**19**) was treated with 4-(dimethylamino)benzaldehyd according to general procedure to give the desired product **24** as a yellow solid, 85% yield. Mp=205.0-205.9□; ^{1}H NMR (400 MHz, $CDCl_3$) δ 7.57 (m, 3H), 7.34 (s, 1H), 6.97 (s, 1H), 6.73 (d, *J* = 8.8 Hz, 2H), 3.99 (s, 3H), 3.94 (s, 3H), 3.90 (s, 2H), 3.04 (s, 6H). ^{13}C NMR (101 MHz, $CDCl_3$) δ 193.29, 154.81, 150.98, 149.45, 144.36, 133.35, 132.45, 131.71, 130.67, 123.44, 111.96, 107.23, 105.04, 56.21, 56.14, 40.08, 32.37; LCMS (APCI) m/z $[(M+H)]^+$ = 324.4; HRMS (ESI) m/z calcd for $C_{20}H_{21}NO_3$, 324.1594. found, 324.1588; Purity: 99.7% (by HPLC).

General procedure for the preparation of 25-37

To a solution of the THP protected indanone (**22**) (261mg, 1mmol) in EtOH (3ml), the appropriate benzaldehyde (1mmol) and 3ml of 4% KOH were added. After stirred at room temperature for 2-5h, the produced light yellow solid was filtered. The solid was dissolved in 10ml EA/butanone (1:1), and treated with 5ml 2M HCl. The mixture was

refluxed for 2h and then concentrated in vacuum. The solid residue was washed with water, and crystallized from methanol.

6-hydroxy-5-methoxy-2-(4-methoxybenzylidene)-2,3-dihydro-1H-inden-1-one (25)

Intermediate **22** was treated with 4-methoxybenzaldehyde according to general procedure to give the desired product **25** as a yellow solid, yield 77%. Mp= 227.0-227.6□; ^{1}H NMR (400 MHz, DMSO-d_6) δ 9.48 (s, 1H), 7.70 (d, J = 8.7 Hz, 2H), 7.36 (s, 1H), 7.16 (s, 1H), 7.12 – 6.99 (m, 3H), 3.93 (s, 2H), 3.91 (s, 3H), 3.83 (s, 3H); ^{13}C NMR (101 MHz, DMSO-d_6) δ 191.96, 160.25, 154.39, 146.89, 143.32, 133.60, 132.25, 130.77, 130.36, 127.70, 114.49, 108.22, 108.05, 55.85, 55.30, 31.46; LCMS (APCI) m/z $[(M-H)]^-$ = 295.3; HRMS (ESI) m/z calcd for $C_{18}H_{16}O_4$, 297.1121. found, 297.1119; Purity: 95.2% (by HPLC).

6-hydroxy-2-(4-hydroxybenzylidene)-5-methoxy-2,3-dihydro-1H-inden-1-one (26)

Intermediate **22** was treated with compounds **7** according to general procedure to give the desired product **26** as a yellow solid, yield 65%. Mp= 278.8-279.5□; ^{1}H NMR (400 MHz, DMSO-d_6) δ 10.07 (s, 1H), 9.52 (s, 1H), 7.58 (d, J = 8.6 Hz, 2H), 7.31 (s, 1H), 7.14 (s, 1H), 7.06 (d, J = 2.4 Hz, 1H), 6.92 – 6.79 (m, 2H), 3.89 (s, 5H).^{13}C NMR (101 MHz, DMSO-d_6) δ 191.99, 158.75, 154.18, 146.69, 143.23, 132.51, 131.25, 130.44, 126.23, 115.92, 115.82, 108.20, 107.93, 99.39, 55.82, 31.51. LCMS

(APCI) m/z $[(M-H)]^-$ =281.3; HRMS (ESI) m/z calcd for $C_{17}H_{14}O_4$, 283.0965. found, 283.0964; Purity: 98.9% (by HPLC).

2-(3,4-dimethoxybenzylidene)-6-hydroxy-5-methoxy-2,3-dihydro-1H-inden-1-one (27)

Intermediate **22** was treated with 3,4-dimethoxybenzaldehyde according to general procedure to give the desired product **27** as a yellow solid, yield 63%. Mp= 177.8-178.4□; ^{1}H NMR (400 MHz, DMSO-d_6) δ 7.35 (s, 1H), 7.30 (d, J = 7.0 Hz, 2H), 7.17 (s, 1H), 7.06 (d, J = 10.9 Hz, 2H), 3.96 (s, 2H), 3.90 (s, 3H), 3.84 (s, 3H), 3.82 (s, 3H); ^{13}C NMR (101 MHz, DMSO-d_6) δ 192.44, 150.60, 149.26, 143.86, 134.17, 131.72, 130.85, 128.40, 124.88, 113.83, 112.36, 108.75, 56.36, 56.05, 55.95, 31.87; LCMS (APCI) m/z $[(M-H)]^-$ =325.4; HRMS (ESI) m/z calcd for $C_{19}H_{18}O_5$, 327.1227. found, 327.1224; Purity: 98.7% (by HPLC).

6-hydroxy-2-(3-hydroxy-4-methoxybenzylidene)-5-methoxy-2,3-dihydro-1H-inden-1-one (28)

Intermediate **22** was treated with compounds **8** according to general procedure to give the desired product **28** as a yellow solid, yield 62%. Mp= 216.2-218.2□; ^{1}H NMR (400 MHz, DMSO-d_6) δ 7.30 (d, J = 13.3 Hz, 2H), 7.23 – 7.11 (m, 2H), 7.07 (s, 1H), 6.88 (d, J = 7.8 Hz, 1H), 3.92 (s, 2H), 3.88 (s, 3H), 3.85 (s, 3H); ^{13}C NMR (101 MHz, DMSO-d_6) δ 191.97, 154.22, 148.38, 147.70, 146.76, 143.23, 132.74, 131.62, 130.44,

126.65, 124.71, 115.80, 114.13, 108.22, 107.99, 55.86, 55.58, 31.43; LCMS (APCI) m/z $[(M-H)]^-$ = 311.3; HRMS (ESI) m/z calcd for $C_{18}H_{16}O_5$, 313.1071. found, 313.1070; Purity: 98.9% (by HPLC).

6-hydroxy-2-(4-hydroxy-3-methoxybenzylidene)-5-methoxy-2,3-dihydro-1H-inden-1-one (29)

Intermediate **22** was treated with compounds **9** according to general procedure to give the desired product **29** as a yellow solid, yield 60%. Mp= 222.9-223.5□; ^{1}H NMR (400 MHz, DMSO-d_6) δ 7.25 (s, 1H), 7.23 – 7.11 (m, 3H), 7.07 (s, 1H), 7.01 (d, J = 8.3 Hz, 1H), 3.89 (s, 3H), 3.87 (s, 2H), 3.82 (s, 3H); ^{13}C NMR (101 MHz, DMSO-d_6) δ 191.93, 154.30, 149.15, 146.81, 146.51, 143.22, 133.40, 131.25, 130.39, 127.97, 123.33, 116.75, 112.17, 108.21, 108.00, 55.83, 55.58, 31.48; LCMS (APCI) m/z $[(M-H)]^-$ = 311.3; HRMS (ESI) m/z calcd for $C_{18}H_{16}O_5$, 313.1071. found, 313.1074; Purity: 98.5% (by HPLC).

2-(4-(dimethylamino)benzylidene)-6-hydroxy-5-methoxy-2,3-dihydro-1H-inden-1-one hydrochloride (30·HCl)

Intermediate **22** was treated with 4-(dimethylamino)benzaldehyde according to general procedure to give the desired product **30** as a yellow solid, yield 65%. Mp= 217.8-219.0□; ^{1}H NMR (400 MHz, DMSO-d_6) δ 9.46 (s, 1H), 7.56 (d, J = 8.9 Hz, 2H), 7.30 (s, 1H), 7.15 (s, 1H), 7.05 (d, J = 2.3 Hz, 1H), 6.78 (d, J = 8.9 Hz, 2H), 3.89

(s, 3H), 3.86 (s, 2H), 2.99 (s, 6H); ^{13}C NMR (101 MHz, DMSO-d_6) δ 191.84, 153.88, 150.88, 146.60, 142.83, 132.21, 131.96, 130.81, 130.62, 122.44, 111.96, 108.24, 107.90, 99.48, 55.81, 31.70; LCMS (APCI) m/z $[(M-H)]^-$ = 308.4; HRMS (ESI) m/z calcd for $C_{19}H_{19}NO_3$, 310.1438. found, 310.1440; Purity: 96.2% (by HPLC).

2-(4-(diethylamino)benzylidene)-6-hydroxy-5-methoxy-2,3-dihydro-1H-inden-1-one hydrochloride (31·HCl)

Intermediate **22** was treated with 4-(diethylamino)benzaldehyde according to general procedure to give the desired product **31** as a yellow solid, yield 83%. Mp= 150.6-151.2□; ^{1}H NMR (400 MHz, DMSO-d_6) δ 7.70 (s, 2H), 7.34 (s, 1H), 7.21-7.18 (m, 2H), 7.14 (s, 1H), 7.08 (s, 1H), 3.91 (s, 2H), 3.89 (s, 3H), 3.49 – 3.47 (m, 4H), 1.08 (t, J = 6.9 Hz, 6H); ^{13}C NMR (101 MHz, DMSO-d_6) δ 191.82, 154.37, 146.86, 143.26, 132.24, 130.43, 108.21, 108.05, 55.87, 47.54, 31.50, 11.19; LCMS (APCI) m/z $[(M-H)]^-$ = 336.4; HRMS (ESI) m/z calcd for $C_{21}H_{23}NO_3$, 338.1751. found, 338.1751; Purity: 99.5% (by HPLC).

2-(4-(ethylamino)benzylidene)-6-hydroxy-5-methoxy-2,3-dihydro-1H-inden-1-one hydrochloride (32·HCl)

Intermediate **22** was treated with 4-(ethylamino)benzaldehyde according to general procedure to give the desired product **32** as a yellow solid, yield 72%. Mp= 237.0-237.7□; ^{1}H NMR (400 MHz, DMSO-d_6) δ 7.61 (d, J = 8.3 Hz, 2H), 7.31 (s, 1H), 7.14 (s, 1H), 7.08 (s, 1H), 6.95 (d, J = 7.7 Hz, 2H), 3.90-3.85 (m, 5H), 3.19-3.10

(m, 2H), 1.21 (t, J = 7.1 Hz, 3H); ^{13}C NMR (101 MHz, DMSO-d_6) δ 191.74, 154.34, 146.95, 143.13, 132.01, 130.47, 108.17, 108.10, 55.85, 31.52, 12.48; LCMS (APCI) m/z $[(M-H)]^-$ = 308.4; HRMS (ESI) m/z calcd for $C_{19}H_{19}NO_3$, 310.1438. found, 310.1431; Purity: 99.8% (by HPLC).

6-hydroxy-5-methoxy-2-(4-(propylamino)benzylidene)-2,3-dihydro-1H-inden-1-one hydrochloride (33·HCl)

Intermediate **22** was treated with 4-(propylamino)benzaldehyde according to general procedure to give the desired product **33** as a yellow solid, yield 75%. Mp= 222.1-222.9□; ^{1}H NMR (400 MHz, DMSO-d_6) δ 7.58 (d, J = 8.2 Hz, 2H), 7.30 (s, 1H), 7.14 (s, 1H), 7.09 (s, 1H), 6.91 (d, J = 7.6 Hz, 2H), 3.90 (s, 3H), 3.89 (s, 2H), 3.10 (t, J = 7.1 Hz, 2H), 1.61 (dd, J = 14.2, 7.2 Hz, 2H), 0.95 (t, J = 7.3 Hz, 3H); ^{13}C NMR (101 MHz, DMSO-d_6) δ 191.75, 154.25, 146.91, 143.04, 132.08, 130.98, 130.53, 108.18, 108.09, 55.87, 31.56, 20.50, 11.23; LCMS (APCI) m/z $[(M-H)]^-$ = 322.4; HRMS (ESI) m/z calcd for $C_{20}H_{21}NO_3$, 324.1594. found, 324.1596; Purity: 99.3% (by HPLC).

2-(4-(cyclohexylamino)benzylidene)-6-hydroxy-5-methoxy-2,3-dihydro-1H-inden-1-one hydrochloride (34·HCl)

Intermediate **22** was treated with 4-(cyclohexylamino)benzaldehyde according to general procedure to give the desired product **34** as a yellow solid, yield 77%. Mp= 250.4-251.0□; ^{1}H NMR (400 MHz, DMSO-d_6) δ 9.57 (s, 1H), 7.46 (d, J = 8.5 Hz,

2H), 7.26 (s, 1H), 7.15 (t, *J* = 13.5 Hz, 2H), 6.67 (d, *J* = 8.5 Hz, 2H), 6.27 (d, *J* = 7.9 Hz, 1H), 3.89 (s, 3H), 3.85 (s, 2H), 1.92 (d, *J* = 9.9 Hz, 2H), 1.73 (d, *J* = 13.0 Hz, 2H), 1.60 (d, *J* = 12.0 Hz, 1H), 1.51 – 0.91 (m, 6H); ^{13}C NMR (101 MHz, DMSO-d_6) δ 191.79, 154.21, 149.21, 146.69, 142.41, 132.51, 132.51, 130.94, 129.61, 122.11, 112.61, 112.22, 108.20, 108.02, 99.22, 55.69, 50.12, 32.39, 32.13, 31.85, 25.32, 24.40, 24.25; LCMS (APCI) m/z $[(M-H)]^-$ =362.4; HRMS (ESI) m/z calcd for $C_{23}H_{25}NO_3$, 364.1907. found, 364.1900; Purity: 95.5% (by HPLC).

2-(4-(dipropylamino)benzylidene)-6-hydroxy-5-methoxy-2,3-dihydro-1H-inden-1-one hydrochloride (35·HCl)

Intermediate **22** was treated with 4-(dipropylamino)benzaldehyde according to general procedure to give the desired product **35** as a yellow solid, yield 80%. Mp= 122.9-123.0□; ^{1}H NMR (400 MHz, DMSO-d_6) δ 7.60 (s, 2H), 7.30 (s, 1H), 7.13 (s, 1H), 7.07 (s, 1H), 7.00 – 6.79 (m, 2H), 3.89 (s, 3H), 3.88 (s, 2H), 3.34 (t, *J* = 7.5 Hz, 4H), 1.67 – 1.36 (m, 4H), 0.88 (t, *J* = 7.3 Hz, 6H); ^{13}C NMR (101 MHz, DMSO-d_6) δ 191.73, 154.20, 146.91, 142.95, 132.24, 130.62, 108.19, 108.09, 55.85, 54.85, 31.57, 19.28, 10.92; LCMS (APCI) m/z $[(M-H)]^-$ = 364.5; HRMS (ESI) m/z calcd for $C_{23}H_{27}NO_3$, 366.2064. found, 366.2078; Purity: 98.9% (by HPLC).

2-(4-(ethyl(methyl)amino)benzylidene)-6-hydroxy-5-methoxy-2,3-dihydro-1H-inden-1-one hydrochloride (36·HCl)

Intermediate **22** was treated with 4-(ethyl(methyl)amino)benzaldehyde according to general procedure to give the desired product **36** as a yellow solid, yield 77%. Mp= 193.7-194.4□; ^{1}H NMR (400 MHz, DMSO-d_6) δ 7.61 (d, J = 8.4 Hz, 2H), 7.32 (s, 1H), 7.15 (s, 1H), 7.07 (s, 1H), 6.93 (s, 2H), 3.92 – 3.87 (m, 5H), 3.49 (dd, J = 13.9, 6.8 Hz, 2H), 2.99 (s, 3H), 1.08 (t, J = 6.9 Hz, 3H); ^{13}C NMR (101 MHz, DMSO-d_6) δ 191.74, 154.30, 146.94, 143.07, 132.14, 130.76, 130.54, 108.21, 108.10, 55.86, 31.54, 10.64; LCMS (APCI) m/z $[(M-H)]^-$ = 322.4; HRMS (ESI) m/z calcd for $C_{20}H_{21}NO_3$, 324.1594. found, 324.1582; Purity: 98.9% (by HPLC).

6-hydroxy-5-methoxy-2-(4-(methyl(propyl)amino)benzylidene)-2,3-dihydro-1H-inden-1-one hydrochloride (37·HCl)

Intermediate **22** was treated with 4-(methyl(propyl)amino)benzaldehyde according to general procedure to give the desired product **37** as a yellow solid, yield 77%. Mp= 133.1-133.8□; ^{1}H NMR (400 MHz, DMSO-d_6) δ 7.57 (d, J = 8.7 Hz, 2H), 7.30 (s, 1H), 7.15 (s, 1H), 7.06 (s, 1H), 6.81 (d, J = 8.2 Hz, 2H), 3.90 (s, 3H), 3.88 (s, 2H), 3.40 – 3.34 (m, 2H), 2.99 (s, 3H), 1.56 (dd, J = 14.5, 7.4 Hz, 2H), 0.89 (t, J = 7.3 Hz, 3H). ^{13}C NMR (101 MHz, DMSO-d_6) δ 192.12, 153.84, 147.28, 142.71, 132.24, 130.59, 108.22, 108.06, 55.83, 31.62, 19.20, 11.02; LCMS (APCI) m/z $[(M-H)]^-$ = 336.4; HRMS (ESI) m/z calcd for $C_{21}H_{23}NO_3$, 338.1751. found, 338.1760; Purity: 98.3% (by HPLC).

General procedure for the preparation of 38-41

TsOH (380mg, 2mmol) was added to a suspension of 5,6-dihydroxy indanone (**20**) (2mmol) and the appropriate benzaldehyde (2mmol) in 10 ml toluene. After refluxed for 10h, the solution was cooled to room temperature. The solid was filtered off, washed with water, and crystallized from methanol.

2-(4-(dimethylamino)benzylidene)-5,6-dihydroxy-2,3-dihydro-1H-inden-1-one 4-methylbenzenesulfonate (38)

5,6-dihydroxy indanone (**20**) was treated with 4-(dimethylamino)benzaldehyde according to general procedure to give the desired product **38** as a yellow solid, yield 71%. Mp= 247.6-248.1□; ^{1}H NMR (400 MHz, DMSO-d_6) δ 7.56 – 7.50 (m, 4H), 7.27 (s, 1H), 7.13 (d, J = 7.7 Hz, 2H), 7.04 (s, 1H), 6.94 (s, 1H), 6.78 (d, J = 8.9 Hz, 2H), 3.81(s, 2H), 2.99 (s, 6H), 2.28 (s, 3H); ^{13}C NMR (101 MHz, DMSO-d_6) δ 191.58, 152.67, 150.80, 145.76, 143.01, 135.74, 132.07, 131.36, 131.07, 130.55, 129.90, 128.97, 125.35, 122.65, 111.97, 111.68, 108.44, 41.59, 31.42, 20.50; LCMS (APCI) m/z $[(M-H)]^-$ = 294.3; HRMS (ESI) m/z calcd for $C_{18}H_{17}NO_3$, 296.1281. found, 296.1276; Purity: 99.7% (by HPLC).

2-(4-(diethylamino)benzylidene)-5,6-dihydroxy-2,3-dihydro-1H-inden-1-one 4-methylbenzenesulfonate (39)

5,6-dihydroxy indanone (**20**) was treated with 4-(diethylamino)benzaldehyde according to general procedure to give the desired product **39** as a yellow solid, yield 67%. Mp= 240.1-240.7□; ^{1}H NMR (400 MHz, DMSO-d_6) δ 10.03 (s, 1H), 9.43 (s, 1H), 7.53 - 7.48 (m, 4H), 7.25 (s, 1H), 7.14 (d, J = 7.6 Hz, 2H), 7.05 (s, 1H), 6.94 (s,

1H), 6.73 (d, *J* = 8.9 Hz, 2H), 3.81 (s, 2H), 3.41 (dd, *J* = 14.0, 7.0 Hz, 4H), 2.32 (s, 3H),1.12 (t, *J* = 7.0 Hz, 6H); ^{13}C NMR (101 MHz, DMSO-d_6) δ 191.64, 152.52, 148.19, 145.73, 142.93, 135.52, 132.47, 131.53, 130.89, 130.45, 130.03, 128.56, 126.17, 121.78, 111.71, 111.32, 108.45, 43.70, 31.45, 20.28, 12.39; LCMS (APCI) m/z $[(M-H)]^-$ = 322.4; HRMS (ESI) m/z calcd for $C_{20}H_{21}NO_3$, 324.1594. found, 324.1595; Purity: 99.5% (by HPLC).

2-(4-(ethyl(methyl)amino)benzylidene)-5,6-dihydroxy-2,3-dihydro-1H-inden-1-one 4-methylbenzenesulfonate (40)

5,6-dihydroxy indanone (**20**) was treated with 4-(ethyl(methyl)amino)benzaldehyde according to general procedure to give the desired product **40** as a yellow solid, yield 66%. Mp= 210.7-211.1□; ^{1}H NMR (400 MHz, DMSO-d_6) δ 7.54-7.51 (m, 4H), 7.27 (s, 1H), 7.10 (d, *J* = 7.8 Hz, 2H), 7.05 (s, 1H), 6.94 (s, 1H), 6.86 (d, *J* = 7.3 Hz, 2H), 3.82 (s, 2H), 3.47 (dd, *J* = 13.8, 6.8 Hz, 2H), 2.98 (s, 3H), 2.29 (s, 3H), 1.08 (t, *J* = 6.9 Hz, 3H); ^{13}C NMR (101 MHz, DMSO-d_6) δ 191.53, 152.92, 145.88, 145.11, 143.23, 137.99, 132.13, 129.75, 128.12, 125.51, 111.71, 108.57, 40.15, 31.32, 20.73, 10.78; LCMS (APCI) m/z $[(M-H)]^-$ = 308.4; HRMS (ESI) m/z calcd for $C_{19}H_{19}NO_3$, 310.1438. found, 310.1426; Purity: 99.0% (by HPLC).

5,6-dihydroxy-2-(4-(methyl(propyl)amino)benzylidene)-2,3-dihydro-1H-inden-1-one 4-methylbenzenesulfonate (41)

5,6-dihydroxy indanone (**20**) was treated with 4-(methyl(propyl)amino)benzaldehyde according to general procedure to give the desired product **41** as a yellow solid, yield 60%. Mp= 222.9-223.1□; ^{1}H NMR (400 MHz, DMSO-d_6) δ 9.98 (s, 1H), 9.35 (s, 1H), 7.53-7.49 (m, 4H), 7.26 (s, 1H), 7.13 (d, J = 7.7 Hz, 2H), 7.05 (s, 1H), 6.94 (s, 1H), 6.76 (d, J = 8.5 Hz, 2H), 3.81 (s, 2H), 3.40 – 3.32 (m, 2H), 2.97 (s, 3H), 2.30 (s, 3H), 1.56 (dd, J = 14.5, 7.2 Hz, 2H), 0.89 (t, J = 7.3 Hz, 3H); ^{13}C NMR (101 MHz, DMSO-d_6) δ 191.62, 152.57, 149.70, 145.75, 145.16, 142.94, 137.92, 132.25, 131.46, 130.70, 129.97, 128.09, 125.51, 122.12, 111.70, 111.61, 108.46, 52.96, 31.44, 20.73, 19.50, 11.13; LCMS (APCI) m/z $[(M-H)]^-$ = 322.2. HRMS (ESI) m/z calcd for $C_{20}H_{21}NO_3$, 324.1594. found, 324.1594; Purity: 97.7% (by HPLC).

Inhibition of Aβ$_{1-42}$ peptide aggregation[23]

Hexafluoro-2-propanol (HFIP) pretreated Aβ$_{1-42}$ samples (Millipore) were dissolved with a 50 mM phosphate buffer (pH = 7.4) in order to have a stable stock solution ([Aβ] = 200μM). The peptide was incubated in 50 mM phosphate buffer (pH = 7.4) at 37 °C for 48 h (final Aβ concentration 50 μM) with or without the tested compound at 20 μM. After incubation, the samples were diluted to a final volume of 200uL with 50 mM glycine-NaOH buffer (pH 8.0) containing thioflavin T. Then, a 300-seconds-time scan of fluorescence intensity was performed (λexc = 450 nm; λem = 485 nm), and values at plateau were averaged after subtracting the background fluorescence of Thioflavin T solution.

The antioxidant activity assay

The antioxidant activity was determined by the oxygen radical absorbance capacity-fluorescein (ORAC-FL) assay. [24,25,26] All the assays were under 75 mM phosphate bufffer (pH 7.4) and the final reaction mixture was 200 μL. Antioxidant (20 μL) and fluorescein (120 μL, 300 nM final concentration) were placed in the wells of a black 96-well plate and the mixture was incubated for 10 min at 37 °C. Then, AAPH (Aldrich) solution (60 μL; 12 mM final concentration) was added rapidly. The plate was immediately placed into a Spectrafluor Plus plate reader (Tecan, Crailsheim, Germany) and the fluorescence was measured every 60 s for 4 h with excitation at 485 nm and emission at 520 nm. Trolox was used as standard (1-10 μM, final concentration). A blank (FL+AAPH) using phosphate buffer instead of antioxidant and Trolox calibration were carried out in each assay. The samples were measured at different concentrations (0.5–10 μM). All reaction mixtures were prepared fourfold and at least four independent runs were performed for each sample. Fluorescence measurements were normalized to the curve of the blank (without antioxidant). The ORAC-FL values were calculated as described in the reference and the final results were in μM of Trolox equivalent/μM of pure compound.

Effects of 41 on $A\beta_{1-42}$ aggregation by TEM Study[28]

$A\beta_{1-42}$ peptide (Millipore) was dissolved in 10 mM phosphate buffer (pH 7.4) at 4°C to give an 80 μM solution. $A\beta_{1-42}$ was incubated in the presence and absence of **41** at

37°C. The final concentrations of both $A\beta_{1-42}$ and **41** were 20μM. At specified time points, aliquots of 10 μL samples were placed on carbon-coated copper/rhodium grid. After 1 min, the grid was washed with water and negatively stained with 2% phosphomolybdic acid solution for 1 min. After draining off the excess of staining solution by means of a filter paper, the specimen was transferred for examination in a transmission electron microscope (JEOL JEM-1400).

Inhibition of MAO activity[29]

The potential effects of the test drugs on hMAO activity were investigated by measuring their effects on the production of H_2O_2 from p-tyramine, using the Amplex Red MAO assay kit (Molecular Probes, Inc) and recombinant human MAO-A or MAO-B (Sigma-Aldrich) corroding to published procedures.

Docking study

The simulation system was built based on the X-ray crystal structure of MAO-B which was obtained from the Protein Data Bank (PDB entry 2Z5X). The original ligand was removed while water molecules present in the PDB file were maintained in their position. 3D structures of the **41** were generated and optimized by Discovery studio 2.1 package (Accelrys Inc., San Diego, CA). The CDOCKER programm Discovery studio 2.1 software was used to perform docking simulations, which allows full flexibility of the ligands.

Metal chelation[30]

Compounds **41** were tested as metal chelators, using difference UV–vis spectra recorded in methanol at 298 K with wavelength ranging from 200 to 600 nm. Numerical subtraction of the spectra of the metal alone and the compound alone from the spectra of the mixture obtained the difference UV-vis spectra due to complex formation. A fixed amount of **41** (50 μM) was mixed with growing amounts of copper ion (5–100μM) and tested the difference UV-vis spectra to investigate the ratio of ligand/metal in the complex.

Effects of 41 on metal-induced $A\beta_{1-42}$ aggregation and Disaggregation experiments by ThT method and TME[28]

HEPES buffer solutions (20 μM) containing 150 μM NaCl were prepared with distilled water at pH values of 6.6. Solutions of Cu^{2+} were prepared from standards to final concentrations of 200 μM using the HEPES buffer at pH 6.6. Solutions of **41** was prepared in DMSO in 10 mM for store, and diluted with HEPES buffer before use. To study effects of **41** on the metal-induced $A\beta_{1-42}$ aggregation, $A\beta_{1-42}$ (50 μM) was incubated 40μM Cu^{2+} in HEPES buffer at pH 6.6, without or with compound **41** (50 μM). The incubation was performed at 37°C for 24 h. After incubation, the samples were diluted to a final volume of 180 μL with 50 mM glycine–NaOH buffer (pH 8.5) containing 5 μ M Thioflavin T. Fluorescence was measured at 450 nm (k_{ex})

and 485 nm (k_{em}) using a monochromators based multimode microplate reader (INFINITE M1000). The TEM study was carried out as the previous procedure.[28]

Disaggregation experiments were carried out according to published procedures.[31,32]

ASSOCIATED CONTENT

Supporting Information: HPLC chromatograms of compounds **23-41**.This material is available free of charge via the Internet at http://pubs.acs.org.

Accession Codes

PDB ID codes: 2Z5X

AUTHOR INFORMATION

Corresponding author. Tel.: +086-20-3994-3050; fax: +086-20-3994-3050; e-mail: lixsh@mail.sysu.edu.cn

ACKNOWLEDGMENT

We thank the Natural Science Foundation of China (20972198) for financial support of this study.

ABBREVIATIONS USED

AD, Alzheimer's disease; Aβ, β-amyloid peptide; MAO-B, monoamine oxidase B; MAO-A, monoamine oxidase A; ACh, acetylcholine; FAD, Food and Drug

Administration; CNS, central nervous system; ROS, reactive oxygen species; MTDLs, multi-target-directed ligands; AChE, acetylcholinesterase; TBAB, Tetrabutylammonium bromide; ThT, Thioflavin T; TEM, transmission electron microscopy; FAD, flavin adenine dinucleotide; PDB, Protein Data Bank; SAR, structure activity relationship.

REFERENCES

1. Scarpini, E.; Schelterns, P.; Feldman, H. Treatment of Alzheimer's disease: current status and new perspectives. *Lancet. Neurol.* **2003**, *2*, 539 - 547.
2. Hardy, J.; Selkoe, D. J. The Amyloid Hypothesis of Alzheimer's Disease: Progress and Problems on the Road to Therapeutics . *Science* **2002**, *297*, 353 - 356.
3. Curtain, C.; Ali, F.; Volitakis, I.; Cherny, R.; Norton, R.; Beyreuther, K.; Barrow, C.; Masters, C.; Bush, A.; Barnham, K. Alzheimer's Disease Amyloid-β Binds Copper and Zinc to Generate an Allosterically Ordered Membrane-penetrating Structure Containing Superoxide Dismutase-like Subunits . *J. Biol. Chem.* **2001**, *276*, 20466 - 20473.
4. Sultana, R.; Perluigi, M.; Butterfield, D. A. Protein Oxidation and Lipid Peroxidation in Brain of Subjects with Alzheimer's Disease: Insights into Mechanism of Neurodegeneration from Redox Proteomics. *Antioxid. Redox. Signal.* **2006**, *8*, 2021 - 2037.

5. Gu, F.; Zhu, M.; Shi, J.; Hu, Y.; Zhao, Z. Enhanced oxidative stress is an early event during development of Alzheimer-like pathologies in presenilin conditional knock-out mice .*Neurosci. Lett.* **2008**, *440*, 44 - 48.

6. Perry, G.; Moreira, P. I.; Santos, M. S.; Oliveira, C. R.; Shenk, J. C.; Nunomura, A.; Smith, M. A.; Zhu, X. Alzheimer Disease and the Role of Free Radicals in the Pathogenesis of the Disease *CNS. Neurol. Disord.–DR.* **2008**, *7*, 3 - 10.

7. Shih, J. C.; Chen, K.; Ridd, M. J. Monoamine Oxidase: From Genes to Behaviour. *Annu. Rev. Neurosci.* **1999**, *22*, 197 - 217.

8. Reinikainen, K. J., Soininen, H., and Riekkinen, P. J. Neurotransmitter changes in Alzheimer's disease: implications to diagnostics and therapy. *J. Neurosci. Res.* **1990**, 27, 576 - 586.

9. Sano, M., Ernesto, C., Thomas, R. G., Klauber, M. R., Schafer, K., Grundman, M., Woodbury, P., Growdon, J., Cotman, C. W., Pfeiffer,E., Schneider, L. S., and Thal, L. J. A Controlled trial of selegiline, alpha-tocopherol, or both as treatment for Alzheimer's disease. *N. Engl. J. Med.* **1997**, *336*, 1216 - 1222.

10. Dong, J.; Atwood, C. S.; Anderson, V. E.; Siedlak, S. L.; Smith, M. A.; Perry, G.; Carey, P. R. Metal binding and oxidation of amyloid-beta within isolated senile plaque cores: Raman microscopic evidence. *Biochemistry* **2003**, *42*, 2768 - 2773.

11. Opazo, C.; Huang, X.; Robert A. C.; Robert D. M.; Alex E. R.; White, A. R.; Roberto, C,; Colin L. M.; Rudolph E. T.; Inestrosa, N. C.; Bush, A. I. Metalloenzyme-like Activity of Alzheimer's Disease β-Amyloid. *J. Biol. Chem.* **2002**, *277*, 40302 - 40308.

12. Huang, X.; Moir, R. D.; Tanzi, R. E.; Bush, A. I.; Rogers, J. T. Redox-Active Metals, Oxidative Stress, and Alzheimer's Disease Pathology. *Ann NY Acad. Sci.* **2004**, *1012*, 153 - 163.

13. Bush, A. I. Drug development based on the metals hypothesis of Alzheimer's disease. *J. Alzheimers. Dis.* **2008**, *15*, 223 - 240.

14. Samadi, A.; Marco-Contelles, J.; Soriano, E.; Alvarez-Perez, M.; Chioua, M.; Romero, A.; Gonzalez-Lafuente, L.; Gandia, L.; Roda, J. M.; Lopez, M. G.; Villarroya, M.; Garcia, A. G.; Delos-Rios, C. Multipotent drugs with cholinergic and neuroprotective properties for the treatment of Alzheimer and neuronal vascular diseases. I. Synthesis, biological assessment, and molecular modeling of simple and readily available 2-aminopyridine-, and 2-chloropyridine-3,5-dicarbonitriles. *Bioorg. Med. Chem.* **2010**, *18*, 5861- 5872.

15. Rosini, M.; Andrisano, V.; Bartolini, M.; Bolognesi, M. L.; Hrelia, P.; Minarini, A.; Tarozzi, A.; Melchiorre, C. Rational approach to discover multipotent anti-Alzheimer drugs. *J. Med. Chem.* **2005**, *48*, 360 - 363.

16. Bolognesi, M. L.; Bartolini, M.; Tarozzi, A.; Morroni, F.; Lizzi, F.; Milelli, A.; Minarini, A.; Rosini, M.; Hrelia, P.; Andrisano, V.; Melchiorre, C. Multitargeted drugs discovery: Balancing anti-amyloid and anticholinesterase capacity in a single chemical entity. *Bioorg. Med. Chem. Lett.* **2011**, *21*, 2655 - 2658.

17. Fernandez-Bachiller, M. I.; Perez, C.; Gonzalez-Munoz, G. C.; Conde, S.; Lopez, M. G.; Villarroya, M.; Garcia, A. G.; Rodriguez-Franco, M. I. Novel Tacrine-8-Hydroxyquinoline Hybrids as Multifunctional Agents for the Treatment

of Alzheimer's Disease, with Neuroprotective, Cholinergic, Antioxidant, and Copper-Complexing Properties. *J. Med. Chem.* **2010**, *53*, 4927 - 4937.

18. Bansal, R.; Narang, G.; Zimmer, C.; Hartmann, R. Synthesis of some imidazolyl-substituted 2-benzylidene indanone derivatives as potent aromatase inhibitors for breast cancer therapy . *Med. Chem. Res.* **2011**, *20*, 661 - 669.
19. Leoni, L. M.; Hamel, E.; Genini, D.; Shih, H.; Carrera, C. J.; Cottam, H. B.; Carson, D. A. Indanocine, a Microtubule-Binding Indanone and a Selective Inducer of Apoptosis in Multidrug-Resistant Cancer Cells. *J. Natl Cancer Inst.* **2000**, *92*, 217 - 224.
20. Sugimoto, H.; Yamanishi, Y.; Iimura, Y.; Kawakami, Y. Donepezil hydrochloride (E2020) and other acetylcholinesterase inhibitors. *Curr. Med. Chem.* **2000**, *3*, 303 - 339.
21. Huang, L.; Shi, A.; He, F.; Li, X. Synthesis, biological evaluation, and molecular modeling of berberine derivatives as potent acetylcholinesterase inhibitors. *Bioorg. Med. Chem.* **2010**, *18*, 1244 - 1251.
22. Huang, L.; Luo, Z. H.; He, F.; Shi, A. D.; Qin, F. F.; Li, X. S. Berberine derivatives, with substituted amino groups linked at the 9-position, as inhibitors of acetylcholinesterase/butyrylcholinesterase. *Bioorg. Med. Chem. Lett.* **2010**, *20*, 6649 - 6653.
23. Rosini, M.; Simoni, E.; Bartolini, M.; Cavalli, A.; Ceccarini, L.; Pascu, N.; McClymont, D.; Tarozzi, A.; Bolognesi, M.; Minarini, A. Tumiatti, V.; Andrisano, V.; Mellor, I.; Melchiorre, C. Inhibition of Acetylcholinesterase,

β-Amyloid Aggregation, and NMDA Receptors in Alzheimer's Disease: A Promising Direction for the Multi-target-Directed Ligands Gold Rush. *J. Med. Chem.,* **2008**, *51,* 4381 - 4384.

24. Ou, B.; Hampsch-Woodill, M.; Prior, R. L. Analysis of Antioxidant Activities of Common Vegetables Employing Oxygen Radical Absorbance Capacity (ORAC) and Ferric Reducing Antioxidant Power (FRAP) Assays: A Comparative Study. *J. Agric. Food Chem.* **2001**, *49*, 4619-4626.
25. Daevalos, A. Extending Applicability of the Oxygen Radical Absorbance Capacity (ORAC−Fluorescein) Assay. *J. Agric. Food Chem.* **2004**, *52*, 48 - 54.
26. Decker, M.; Kraus, B.; Heilmann, J. Design, synthesis and pharmacological evaluation of hybrid molecules out of quinazolinimines and lipoic acid lead to highly potent and selective butyrylcholinesterase inhibitors with antioxidant properties. *Bioorg. Med. Chem.* **2008**, *16*, 4252 - 4261.
27. Hubalek, F.; Binda, C.; Li, M.; Herzig, Y.; Sterling, J.; Youdim, M. B. H.; Mattevi, A.; Edmondson, D. E. Inactivation of Purified Human Recombinant Monoamine Oxidases A and B by Rasagiline and Its Analogues. *J. Med. Chem.* **2004**, *47*, 1760 - 1766.
28. Chen, S.; Chen. Y.; Li, Y.; Chen. S.; Tan, J.; Ou, T.; Gu. L.; Huang. Z. Design, synthesis, and biological evaluation of curcumin analogues as multifunctional agents for the treatment of Alzheimer's disease. *Bioorg. Med. Chem.* **2011**, *19*, 5596 - 5604.

29. Chimenti, F.; Secci, D. Bolasco, A.; Chimenti, P.; Bizzarri, B.; Granese, A.; Carradori, S.; Yanez, M.; Orallo, F.; Ortuso, F.; Alcaro, S. Synthesis, Molecular Modeling, and Selective Inhibitory Activity against Human Monoamine Oxidases of 3-Carboxamido-7-Substituted Coumarins. *J. Med. Chem.* **2009**, *52*, 1935-1942.

30. Huang, W. H.; Lv, D.; Yu, H. P.; Sheng, R.; Kim, S. C.; Wu, P.; Luo, K. D.; Li, J.; Hu, Y. Z. Dual-target-directed 1,3-diphenylurea derivatives: BACE 1 inhibitor and metal chelator against Alzheimer's disease. *Bioorg. Med. Chem.* **2010,** *18*, 5610-5615.

31. Hindo, S.; Mancino, A.; Braymer, J.; Liu, Y.; Lim, M. Small molecule modulators of copper-induced Aβ aggregation. *J. Am. Chem. Soc.* **2009**, *131*, 16663 - 16665.

32. Choi, J.; Braymer, J.; Nanga, R.; Ramamoorthy, A.; Lim, M. Design of small molecules that target metal-Aβ species and regulate metal-induced Aβ aggregation and neurotoxicity. *Proc. Natl. Acad. Sci. U.S.A.* **2010**, *107*, 21990 - 21995.

Table of Contents graphic

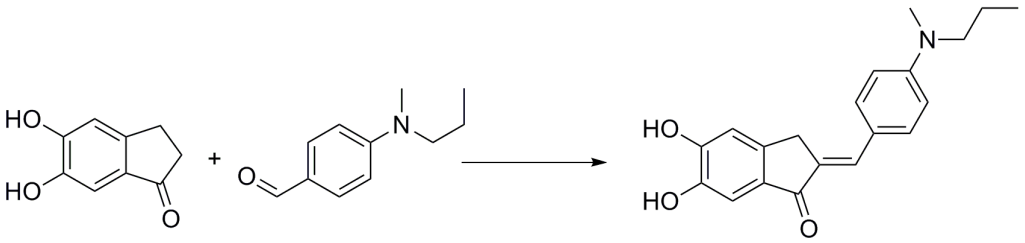

Anti-Aβ aggregation: 80.1% at 20 μM
ORAC-FL value of 5.60 (Trolox equiv)
MAO-B IC_{50}: 7.50μM